Tunable RF Front-end Filter with Wideband Blocker Suppression for Multi-Standard Applications

M. Naimul Hasan and Xiaoguang Liu
School of Electrical and Computer Engineering, University of California Davis, California, USA
Email: mhasan@ucdavis.edu

***Abstract*—This paper presents a tunable active bandpass filter with bandwidth-adjustable notches close to the passband for wideband blocker suppression with high attenuation. The proposed filter is composed of a 3-pole N-path bandstop filter in cascade with an N-path bandpass filter, where the center frequency of the bandpass filter is offset from the bandstop filters. With proper tuning of the coupling capacitors in the bandstop filter, three adjacent notches can be created which provides a larger suppression bandwidth. An implementation of the filter in 65-nm CMOS exhibits a passband tunable between 0.1–1.1 GHz, with a 3-dB bandwidth of 12.4–14.2 MHz, a gain of 9.5–10.3 dB, a noise figure of 4.3–5.8 dB, and a total power consumption of 40–64.3 mW. The blocker 1-dB compression point is 6.5 dBm and the out-of-band IIP3 is 18.4 dBm. The reported filter provides a promising solution to multi-standard, multi-frequency software-defined radio applications.**

***Index Terms*—Bandpass filter, blocker rejection, CMOS, N-path, notch filter, Switched-capacitor, transmitter leakage.**

I. Introduction

In order to efficiently utilize the limited frequency spectrum as well as to increase the data rate in wireless communications, aggregating two or more adjacent or non-adjacent RF channels (carrier aggregation) is proposed in long-term evolution (LTE)-advanced standard [1]. However, the higher data rate and more flexibility in spectrum utilization come at the cost of more susceptibility to interferences from friendly and unfriendly sources.

Various on-chip techniques to handle out-of-band blockers have been proposed recently [2]–[4]. A combination of bandpass (BP) and bandstop (BS) filters have been proposed in [2], [4] to create notches close to the passband. Although these approaches are suitable for suppressing a single frequency blocker, the created single-frequency notch is not effective in presence of wideband blockers which is becoming more prevalent with the development in high-speed wireless communications.

In this paper, a tunable bandpass filter with a wideband notch is proposed. The proposed filter consists of a 3-pole BS filter along with a 1-pole bandpass filter as shown in Fig. 1(a) and the transfer function of the filter is shown in Fig. 1(b). The center frequency of the BS filter is set by the local oscillator (LO) and the center frequency of the bandpass filter is shifted to an offset frequency.

II. Wideband Notch Creation

A conventional 3-pole bandstop filter is shown in Fig. 2(a). Gyrators can be used to transform series LC resonators (L_1, C_1 and L_3, C_3) to parallel LC resonators [2]. The schematic of

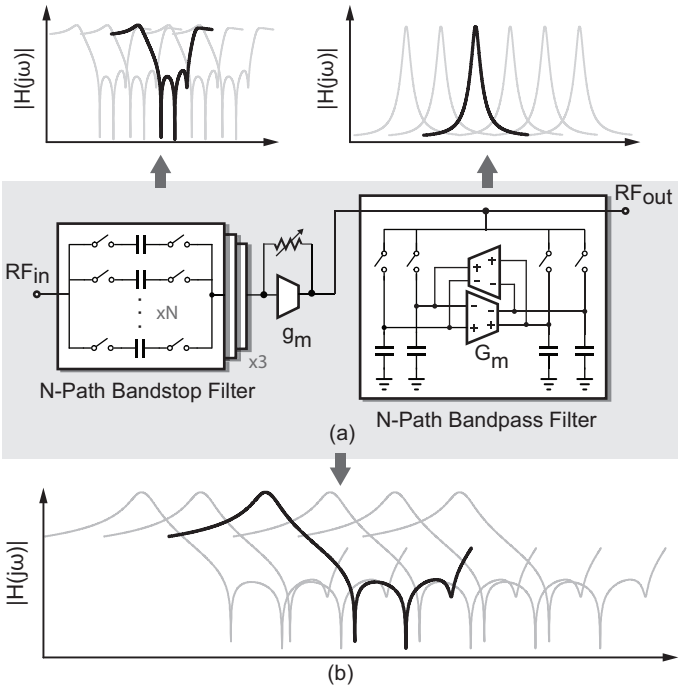

Fig. 1: (a) Proposed bandpass filter with wideband notch creation. (b) The filter creates a 50 MHz wideband notch with 40 dB rejection.

the bandstop filter used in the proposed architecture is shown in Fig. 2(b). The coupling capacitors, C_{b1} and C_{b2} are used instead of using the full gyrator implementation. To isolate the first and third resonator center frequency, a different coupling capacitor is used, which means $C_{b1} \neq C_{b2}$. The filter shown in Fig. 2(b) is composed of 3 impedances Z_1, Z_2 and Z_3. The notch frequencies can be easily find when $Z_1, Z_3 \rightarrow 0$ and $Z_2 \rightarrow \infty$. Based on this understanding, the notch frequencies will be located at $\omega_{z1} = 1/\left[L_2(C_2' + C_{b1})\right]$, $\omega_{z2} = 1/L_2C_2$, and $\omega_{z3} = 1/\left[L_2(C_2' + C_{b2})\right]$. Fig. 2 (c) shows the simulated transfer function of a 1-GHz wideband bandstop filter in comparison with a conventional multi-pole bandstop filter. The proposed filter shows 30 MHz extra BW compared with all-pole filter for 40 dB rejection.

III. N-Path Implementation of the Filter

The detailed schematic of the proposed filter is shown in Fig. 3. The parallel LC tanks are implemented with shunt configuration of N-path filter. The center frequency of the bandpass filter is shifted with respect to the switching frequency f_{LO} by using g_m-C technique as illustrated in [5].

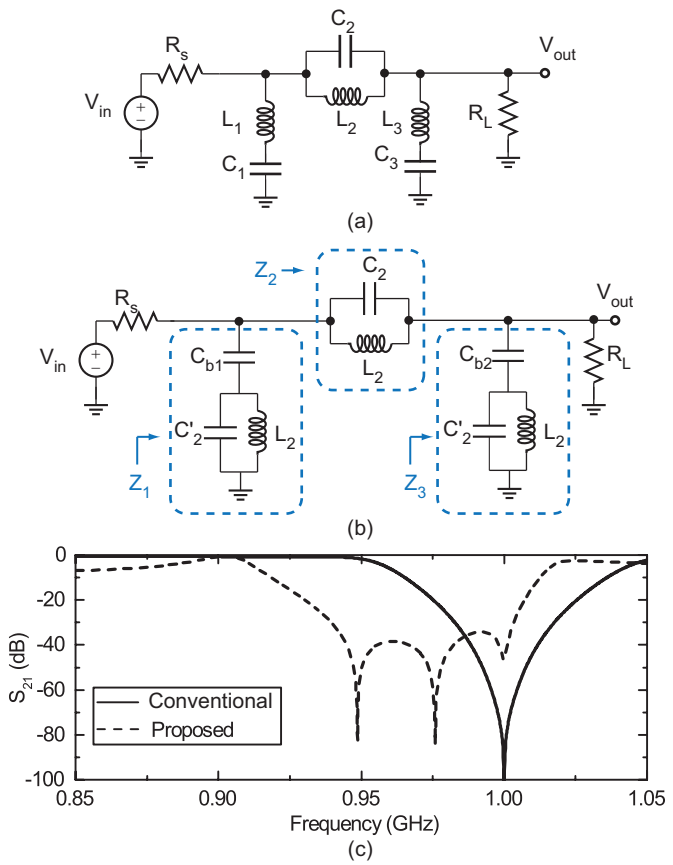

Fig. 2: (a) A conventional 3-pole bandstop (BS) filter. (b) Series LC tanks (L_1, C_1, L_3 and C_3) are transformed to a parallel LC tanks by using capacitive coupling. (c) A comparison of the proposed filter performance with a 3-pole conventional bandstop filter.

The frequency shift $\omega_{shift} = G_m/C_{BP}$ is determined by g_m cells and the baseband capacitance C_{BP}. The frequency can be shifted in both directions (upward or downward) by flipping the connection in the g_m cells used in bandpass resonators. To increase the frequency shifting, either g_m needs to be increased (increases the power consumption) or reduce the baseband capacitance (increases the filter bandwidth).

Two g_m cells are used after the bandstop filter to provide gain and isolate both sections. The first g_m cell along with the tunable feedback resistance provides gain as well as input impedance matching and reduce the noise from subsequent stages. The second g_m stage is set only for providing the necessary gain. The first g_m cell is based on a self-biased inverter unit cell [2]. Other g_m cells are shown in Fig. 3(b–c). The second g_m cell is made tunable to maintain the overall gain of the filter constant.

Following the procedure in [2], Z_{in} of the filter at the resonant frequency f_s can be found assuming $C_{BB1} = C_{BB3}$

$$Z_{in}(s) \simeq (R_{sw} + \frac{1}{sC_{b1}} + k_1)||(R_{sw} + k_2 + P), \quad (1)$$

where

$$k_1 = \frac{N}{\pi^2}\sin^2\left(\frac{\pi}{N}\right)\times[Z_{BB1}(s - j\omega_{LO}) + Z_{BB1}(s + j\omega_{LO})]\,,$$

$$k_2 = \frac{N}{\pi^2}\sin^2\left(\frac{\pi}{N}\right)\times[Z_{BB2}(s - j\omega_{LO}) + Z_{BB2}(s + j\omega_{LO})]\,,$$

$$P = \left(R_{sw} + \frac{1}{sC_{b2}} + k_1\right)||\left(\frac{R_{f1}}{1 + g_{m1}r_{o1}}\right), \quad (2)$$

where Z_{BB1} and Z_{BB2} are the baseband impedances corresponding to the capaciatnce C_{BB1} and C_{BB2} respectively. r_{o1} is the output impedance of the first g_m cell. The coupling capacitors C_{b1}, C_{b2} and the first g_m cell have impact on the input impedance matching as shown in (1). C_{b1} and C_{b2} determine the notch frequency and the overall notch bandwidth. As a result, there is a trade-off between reflection co-efficient (S_{11}) and notch bandwidth. C_{b1} and C_{b2} are chosen carefully for desired notch bandwidth and the S_{11} is primarily controlled by g_{m1} and R_{f1} .

NMOS switches of W/L=80 µm/60 nm are driven by 25% duty cycle 4-phase clocks used in both bandpass and bandstop filters. Large switches are used to reduce their noise, non-linearity and mismatch between them. The switches are biased at 900-mV DC voltage to provide full 1.2-V swing to maximize the linearity of the switches. MIM capacitors with underlying metal are used for the baseband capacitors. The resistors are realized with N+ poly resistor without salicide.

IV. Measurement Results

The proposed filter is realized in 65 nm CMOS technology. The measured transfer function of the filter as well as the reflection parameters (S_{11}) over the whole tuning range is shown in Fig. 4(a). The notch frequency is tuned by changing the LO frequency and the coupling capacitors (C_{b1} and C_{b2}). A close-up of the measured transfer function of the filter with $f_{LO} = 1$ GHz is shown in Fig. 4(b).

The filter has 10-dB gain provided by the g_m cells and a notch bandwidth of 25 MHz for 30 dB rejection (from maximum gain to notch depth). The center frequency of the bandpass filter is 100 MHz offset from the notch center frequency in these measurements.

The noise figure (NF) of the filter over the tuning range is shown in Fig. 5(a) and the NF with different blocker power level is shown in Fig. 5(b) with $f_{LO} = 1$ GHz. In this test, the blocker was located at the LO frequency.

The two-tone test to measure the IIP3 is shown in Fig. 6(a). The tones are located at 1.004 GHz and 1.005 GHz for the in-band IIP3 measurement and the tones are located at 1.05 GHz and 1.105 GHz for the out-of-band IIP3 measurement. The parasitic capacitance at each node of the filter modifies the equivalent resistance of that node. As a result, the Q-factor of the filter increases as the clock frequency reduces.

The chip micrograph of the filter is shown in Fig. 6(b) with total area of 1.1 mm^2 including bonding pads. The proposed filter is compared with the state-of-the-art receivers and filters in Table-I.

V. Conclusion

A tunable bandpass filter with wideband notch is presented in this paper for multi-standard applications. Due to the tunability of the notch frequencies, the proposed filter can

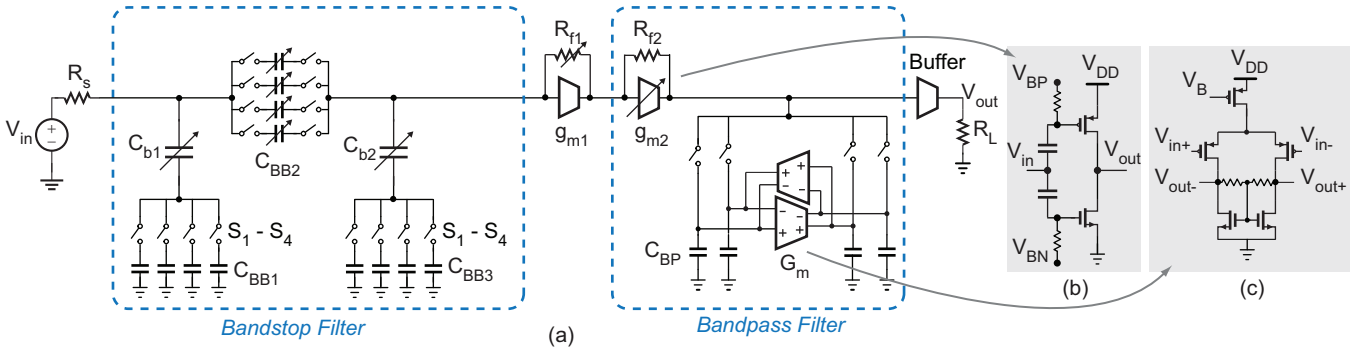

Fig. 3: (a) The complete schematic of the proposed filter. (b) The g_{m2} cell, and (c) differential G_m cells .

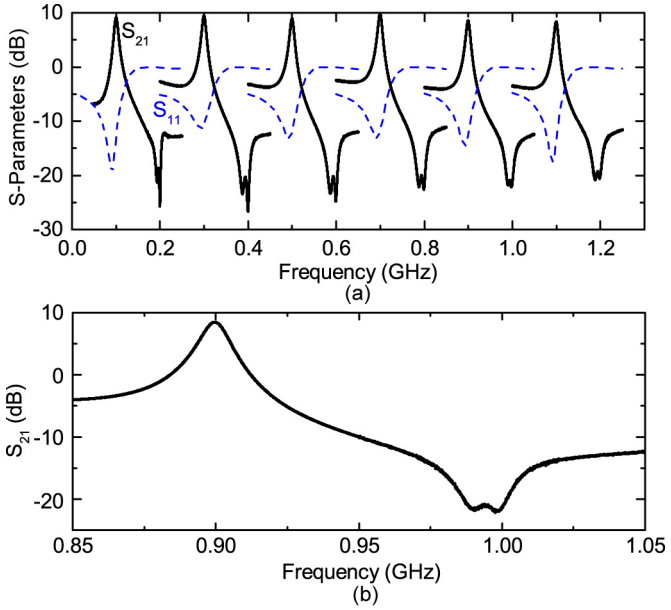

Fig. 4: (a) Measured S_{21} and S_{11} of the fabricated filter in the range of 0.1–1.1 GHz. (b) Measured filter response with $f_{LO} = 1$ GHz.

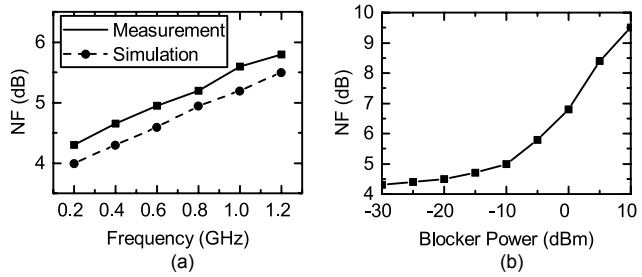

Fig. 5: (a) Measured NF of the proposed filter over the tuning range. (b) Measured NF with different blocker power at 1 GHz.

handle strong dynamic blockers close to the passband and as such show promises as front-end filters for software-defined radio applications.

REFERENCES

[1] "3GPP TS 36.300 v 12.6.0, June 2015; technical specification group radio access network; e-utra and e-utran; overall description; stage 2, release 12."

[2] M. N. Hasan, Q. J. Gu, and X. Liu, "Tunable blocker-tolerant on-chip radio-frequency front-end filter with dual adaptive transmission zeros for software-defined radio applications," *IEEE Transactions on Microwave Theory and Techniques*, vol. 64, no. 99, pp. 1–15, Dec. 2016.

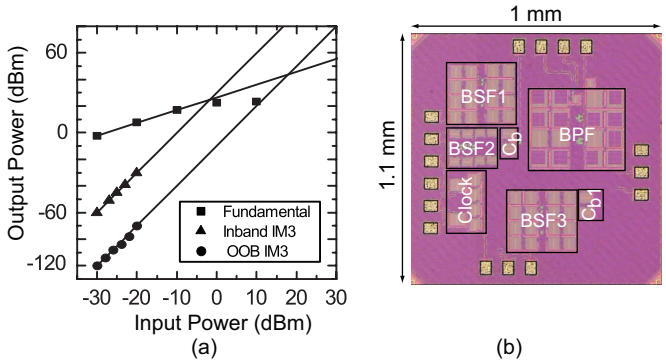

Fig. 6: (a) Measured out-of-band IIP3 and in-band IIP3 at 1 GHz. (b) Chip micrograph of the proposed filter.

TABLE I: Comparison table

	Luo [6]	Naimul [2]	Chen [3]	This work
Circuit Type	LNA	Filter	Receiver	Filter
CMOS Tech (nm)	32 [SOI]	65	65 [LP]	65
Tuning range (GHz)	0.4–6	0.1–1.4	0.5–3	0.1–1.1
Gain (dB)	10	23	38	10.3
BW (MHz)	15	10.2	1 ∼ 30	12.4–14.2
Maximum notch depth[1](dB)	35	50	20	40
30-dB Notch bandwidth (MHz)	10	15	5	25
NF [dB]	3.6–4.9	3–4.2	3.8–4.7	4.3–5.8
Blocker P1dB [dBm]	17	8	-1	6.5
IIP3 (OOB) [dB]	36	23	10	18.4
Area[2]	0.88	2.4	7.8	1.1
Power [mW]	81–209	50–73	76–96	40–64.3

[1]From maximum gain to notch depth. [2] Including bonding pads.

[3] R. Chen and H. Hashemi, "Reconfigurable receiver with radio-frequency current-mode complex signal processing supporting carrier aggregation," *IEEE Journal of Solid-State Circuits*, vol. 50, no. 12, pp. 3032–3046, Dec. 2015.

[4] ——, "Dual-carrier aggregation receiver with reconfigurable front-end RF signal conditioning," *IEEE Journal of Solid-State Circuits*, vol. 50, no. 8, pp. 1874–1888, Aug. 2015.

[5] M. Darvishi, R. van der Zee, E. A. M. Klumperink, and B. Nauta, "Widely tunable 4th order switched Gm -C band-pass filter based on N-path filters," *IEEE Journal of Solid-State Circuits*, vol. 47, no. 12, pp. 3105–3119, Dec. 2012.

[6] C. K. Luo, P. S. Gudem, and J. F. Buckwalter, "A 0.4-6-GHz 17–dBm B1db 36–dBm IIP3 channel-selecting low-noise amplifier for SAW-less 3G/4G FDD diversity receivers," *IEEE Transactions on Microwave Theory and Techniques*, 2016.